Detecting determinism in short time series using a quantified averaged false nearest neighbors approach

Sofiane Ramdani*
EA 2991 Efficience et Déficience Motrices, Université de Montpellier I, Montpellier, France

Frédéric Bouchara
UMR CNRS 6168 LSIS, Université du Sud Toulon-Var, La Garde, France

Jean-François Casties
EA 2991 Efficience et Déficience Motrices, Université de Montpellier I, Montpellier, France

(Received 27 April 2007; revised manuscript received 12 July 2007; published 12 September 2007)

We propose a criterion to detect determinism in short time series. This criterion is based on the estimation of the parameter E_2 defined by the averaged false neighbors method for analyzing time series [Cao, Physica D **110**, 43 (1997)]. Using surrogate data testing with several chaotic and stochastic simulated time series, we show that the variation coefficient of E_2 over a few values of the embedding dimension d defines a suitable statistic to detect determinism in short data sequences. This result holds for a time series generated by a high-dimensional chaotic system such as the Mackey-Glass one. Different decreasing lengths of the time series are included in the numerical experiments for both synthetic and real-world data. We also investigate the robustness of the criterion in the case of deterministic time series corrupted by additive noise.

DOI: 10.1103/PhysRevE.76.036204 PACS number(s): 05.45.Tp, 05.45.Ac

I. INTRODUCTION

During the two last decades, nonlinear determinism has become a powerful paradigm for the analysis of many dynamical behaviors in different research fields from biology to optics. In this framework, one of the most investigated aspects is nonlinear time series analysis and detection of determinism in irregular and complex experimental signals. Among many different approaches that aim to analyze the underlying dynamical process of a time series, the phase space reconstruction (PSR) based ones have been extensively studied. The concept of PSR was first numerically demonstrated by Packard *et al.* [2] and then mathematically proved by Takens [3]. In the case of deterministic times series, it has been shown that the PSR technique leads to estimation of the embedding dimension [4] and dynamical invariants such as the correlation dimension [5], Lyapunov exponents [6–9], or different entropy quantities [10–12] (see also [13] and [14] for an overview of related nonlinear data processing techniques).

More generally, the PSR technique is also the basis of several approaches to distinguish stochastic time series from purely deterministic ones. For example, Sugihara and May [15] proposed to use short-term prediction techniques to detect determinism. A similar approach, based on the estimation of the nonlinear prediction error, was used by Tsonis and Elsener [16] to identify chaotic behaviors. Kennel and Isabelle [17] also used a nonlinear prediction criterion by comparing the given data to an ensemble of random control data sets.

Other methods used to distinguish chaos from noise are based on the observation that the reconstructed trajectories generated by an underlying chaotic dynamical systems are smooth and differentiable. This is not the case for signals produced by stochastic processes. Following this idea, Kaplan and Glass [18] proposed to measure the average directional vectors in a coarse-grained d-dimensional embedding of the time series. The algorithm seems to be efficient for short time series (655 points) in the case of low-dimensional chaotic time series. One year later, Wayland *et al.* [19] proposed a computationally efficient variant of the Kaplan-Glass method. The shortest simulated time series were 1024 points in length. This method requires arbitrary choices of input parameters, such as the number of nearest neighbors and the number of random centers. No output parameter is defined by this method in order to achieve statistical tests. However, the results of the method were qualitatively and successfully compared to those of the amplitude-adjusted Fourier transform (AAFT) surrogate time series using the approach of Theiler *et al.* [20]. Salvino and Cawley [21] also exploited the continuity criterion and defined a smoothness detector to test the determinism of a time series. The authors validated their method on simulated data obtained from the Hénon, Lorenz, and Rössler attractors. The algorithm was applied to time series of lengths 20 000, 3000, and 500 points. The AAFT surrogate data testing method [20] was adapted and performed to assess the validity of the criterion but no stochastic time series were included in the numerical experiments. In this approach, and similarly to the Kaplan-Glass one, the criterion depends on an arbitrary choice of the embedding dimension and the PSR lag time is used as a variable input parameter. The choice of the number and size of the coarser grid boxes used is also arbitrary. In addition, the method is dependent on the vector field used to define the proposed statistic. A modified version of this algorithm was proposed by Jeong *et al.* [22] to investigate the dynamics of long recorded electroencephalogram time series. Ortega and

*sofiane.ramdani@univ-montp1.fr

Louis [23,24] proposed another approach also based on the smoothness principle. Note that the statistic used in these papers is dependent on the chosen embedding dimension for the PSR. Another important input parameter is the ball radius used to estimate the density defined by the time series in the reconstructed phase space. A similar method was later applied to detect determinism in high-dimensional systems [25].

Jeong *et al.* [26,27] proposed another approach also based on the smoothness that characterizes the reconstructed trajectories of deterministic systems. The method is based on the computation of the angles between two successive tangent vectors in the PSR trajectory as a function of time (see Fig. 1). A statistic [the central tendency measure (CTM)] is also derived to distinguish purely deterministic time series from random ones. Moreover, an improved version of the AAFT surrogates was used to perform statistical tests (with 20 surrogates generated for each tested time series). Such surrogates are called iteratively refined AAFT (IAAFT) surrogates and were introduced by Schreiber and Schmitz [28]. In these papers, the authors focused on short time series (2000 point length for the simulated ones and at least an average of 1525 for the experimental ones). From a purely methodological point of view, we can point out that this method applies for data satisfying a weak stationarity condition. In addition, the embedding parameters (the dimension and lag time of the PSR procedure) are needed to estimate the CTM statistic. The authors used parametric *t*-tests to achieve a statistical comparison between the original CTM's and those of the surrogate data. Generally, nonparametric tests are recommended for such data-processing techniques [13,20,29] as the Gaussian assumption for the distribution of the tested statistic does not always hold.

One can also find in the literature alternative methods for detecting determinism that are not based on the smoothness principle [30–32]. All these approaches were validated on relatively short time series (with 1000 to 2000 samples) and generally require several input parameters.

A different approach for detecting determinism is the so-called global false nearest neighbors (FNN) one [4]. This method was designed to determine a correct embedding dimension which allows the reconstruction of the possible attractor of the system. In this approach, a criterion to determine the percentage of false neighbors is defined for a given time-delay vector obtained for different embedding dimensions. If the embedding dimension is too low, this percentage is increased due to the geometrical projection phenomenon. When the percentage is computed for different embedding dimensions, it decreases continuously and a minimum value (close to zero) is reached, which means that the dimension is large enough to describe the dynamics. In the case of a stochastic process, the theoretical percentage of false neighbors does not decrease continuously as the embedding is increased. It has an irregular behavior. Unfortunately and even though some recommendations are given in [4,14], the FNN algorithm uses a subjective parameter, namely, the threshold R_{tol} that defines whether the neighbor of a given time delay vector is false or not. The classical threshold choice ranges from 5 to 20. Figure 2 shows an example of the application of the FNN method to a 1000-sample time series generated by the Ikeda map.

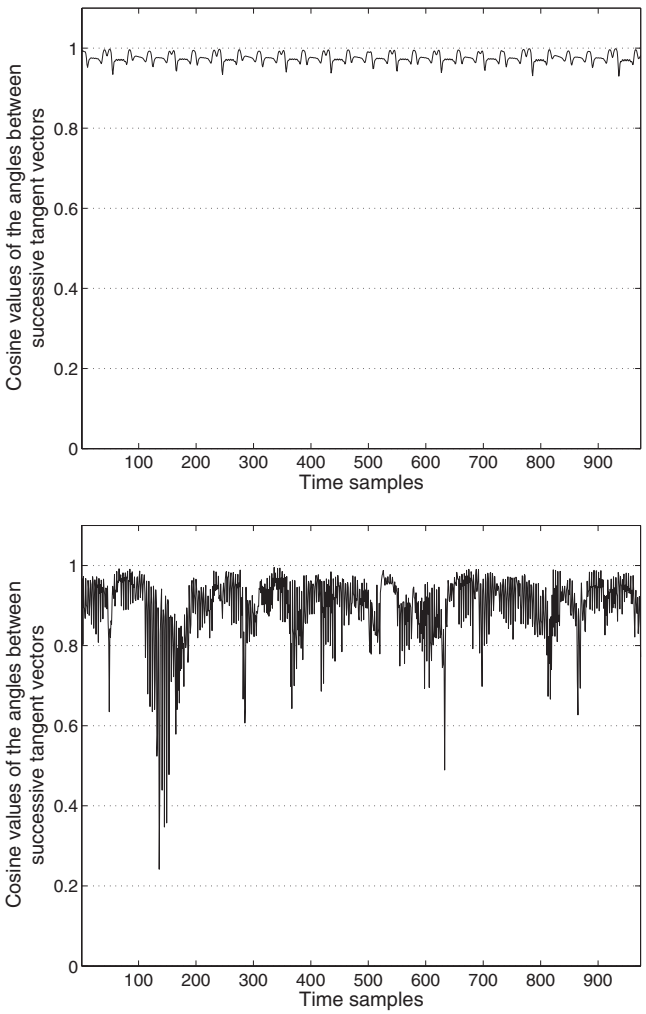

FIG. 1. Cosine values of the angles between successive tangent vectors obtained from a PSR performed on a 1000-point Lorenz time series (upper frame). The embedding dimension is set to 7 and the lag time is 4. A similar figure obtained for an iteratively refined surrogate of the same time series is shown in the lower frame. In this case, the CTM for the original time series is 0.0053. The surrogate CTM is 0.1071. The CTM quantifies the irregularity of the cosine fluctuations. The smoothness of the Lorenz system implies cosine values that are close to 1 with very weak irregularity. The surrogate procedure adds a random component which creates important fluctuations of the cosine values.

Some authors [33–38] analyzed the FNN algorithm or proposed more sophisticated variants of the method to investigate the deterministic nature of time series corrupted by noise but did not really solve the threshold problem. Hegger and Kantz [39] published a very interesting paper in which they proposed an improvement of the FNN method. The threshold issue is addressed. Unlike what is done in most applications of the method, the authors suggest to explore the behavior of the algorithm with different values of the threshold. They also pointed out that the minimal reasonable threshold is given by the maximum of the local deterministic expansion rate, which can be much larger than the expansion factor $e^{\tau\lambda_{max}}$ (where λ_{max} is the largest Lyapunov exponent and τ the lag time of the PSR). This aspect of the algorithm

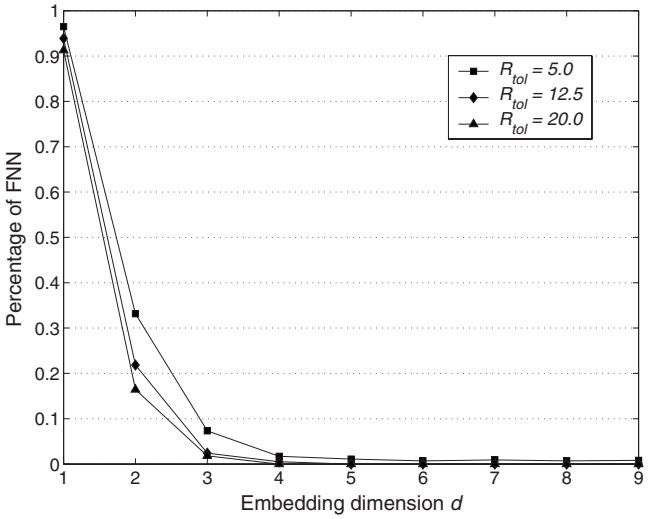

FIG. 2. Percentage of FNN's as a function of the embedding dimension d obtained with a 1000-point Ikeda time series. The choice of the threshold R_{tol} has an important influence on the behavior of the method.

is still under discussion. In addition, the authors showed in this paper that the FNN algorithm has to be combined with surrogate data tests (based on IAAFT surrogates) in order to ensure a correct distinction between low-dimensional chaotic data and noise.

To avoid this subjective choice of the threshold, Cao proposed a modified algorithm [1] sometimes called the averaged false neighbors (AFN) method. Cao's approach is based on the estimation of two parameters E_1 and E_2 which are basically derived from quantities that are defined by the FNN method. These parameters are computed for different increased values of the embedding dimension d. Then the global behaviors of E_1 and E_2 as functions of d are respectively used to estimate the minimum embedding dimension and to determine the nature (stochastic vs deterministic) of the underlying dynamical process generating the time series. This method has many advantages: it does not need too long time series (in the original paper [1] it was applied to a 1000-point time series), it is computationally efficient, and some of its features are not very sensitive to noise [40]. Moreover, it is not based on any arbitrary choice of a threshold. It requires only the determination of the time delay (or lag time) of the PSR procedure, which can be estimated reliably using the average mutual information (AMI) approach [41]. In [38], the E_1 parameter was analyzed to improve the efficiency of the AFN method for the estimation of the minimum embedding dimension of low-dimensional chaotic attractors (Lorenz and Rössler) in the presence of additive white uniform and Gaussian noises. In this paper, the simulated time series were 30 000 points in length.

The main disadvantage of the AFN method is that it is based on the observation of the curves defined by $E_1(d)$ and $E_2(d)$, which is somewhat subjective. Therefore, the algorithm has no quantified output that can be used in a comparative manner or to establish a statistical test in order to detect determinism in a time series.

In the present work, we will focus on the parameter E_2 used as an indicator of the nature of the underlying dynamical system. Its qualitative variations as function of the embedding d have been shown [1,40] to be able to distinguish random behaviors from purely deterministic ones. After computing the value of $E_2(d)$ for some values of d, we propose to derive a simple statistical parameter, namely, a variation coefficient V_{E_2}. Using an IAAFT surrogate data-testing approach [20,28,29], we show that this parameter defines a suitable criterion to distinguish stochastic time series from deterministic ones. The numerical experiments are performed on several simulated chaotic data (from the Hénon, Ikeda, Lorenz, and Rössler attractors and the Santa Fe competition experimental laser time series) and stochastic time series (white Gaussian noise and colored noises). Moreover, the effect of data length is investigated by decreasing the number of available samples from 1000 down to 250. The robustness of the criterion is tested for purely deterministic time series corrupted by an increasing level of additive noise. Then, we investigate the behavior of the V_{E_2} statistic for a high-dimensional chaotic system: the Mackey-Glass one. Finally, an experimental human postural sway time series is included to conclude these numerical experiments.

The next section is devoted to the presentation of the AFN method and briefly discusses interpretation of its results. Section III describes the proposed statistic derived from the parameter E_2 in order to achieve a comparison with the IAAFT surrogate time series. The following section gives the details of the numerical experimental procedure used to assess the criterion. Finally, in Sec. V, we discuss the results of the simulations.

II. THE AFN ALGORITHM

The method is first based on the construction of the time-delay vectors from the time series $x_1, x_2, \ldots, x_N$. The d-dimensional vector is defined by

$$y_i(d) = (x_i, x_{i+\tau}, \ldots, x_{i+(d-1)\tau}) \tag{1}$$

with $i = 1, 2, \ldots, N-(d-1)\tau$, where τ is the time delay.

Similarly to the FNN method [4,14] the AFN approach [1] defines the quantity

$$a(i,d) = \frac{\|y_i(d+1) - y_{n(i,d)}(d+1)\|}{\|y_i(d) - y_{n(i,d)}(d)\|} \tag{2}$$

where $\|.\|$ is the maximum norm and $n(i,d)$ is an integer such that the d-dimensional time-delay vector $y_{n(i,d)}(d)$ is the nearest neighbor of $y_i(d)$.

The next step of the AFN method is to define the averaged quantity

$$E(d) = \frac{1}{N - d\tau} \sum_{i=1}^{N-d\tau} a(i,d). \tag{3}$$

The definition of the first parameter E_1 is then given by

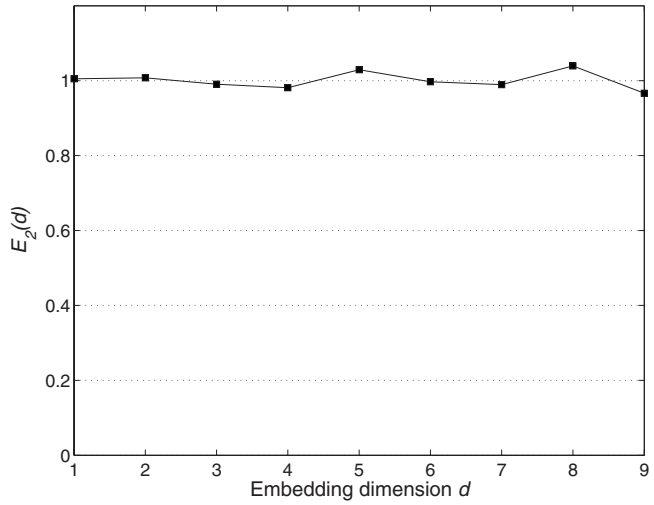

FIG. 3. AFN parameter E_2 as a function of the embedding dimension obtained with a 1000-point WGN time series (with lag time $\tau=1$).

$$E_1(d) = \frac{E(d+1)}{E(d)}. \tag{4}$$

By increasing the value of d, this first parameter is increased, and it stops changing when the time series comes from a deterministic process. If a plateau is observed for $d \geq d_0$ then d_0 is the minimum embedding dimension.

The AFN method also stated a second quantity E_2 which is the useful one to distinguish stochastic processes from purely deterministic ones:

$$E_2(d) = \frac{E^*(d+1)}{E^*(d)} \tag{5}$$

with

$$E^*(d) = \frac{1}{N - d\tau} \sum_{i=1}^{N-d\tau} |x_{i+d\tau} - x_{n(i,d)+d\tau}|. \tag{6}$$

In the original paper it is suggested that theoretically, for random processes, E_2 is independent of d and always equal to 1. Conversely, for purely deterministic time series it cannot be constant for all d. Figures 3–6 show the variations of E_2 against the embedding dimension d for several typical simulated time series generated by random processes and chaotic attractors.

III. THE PROPOSED AFN CRITERION FOR DETECTING DETERMINISM

In the original paper [1], many numerical experiments were performed and confirmed the expected results for the parameter E_2. Several simulated time series were tested, including data obtained from the Hénon, the Ikeda, and the Lorenz attractors, and also a colored noise data set. However, the only justification for the expected results was quite intuitive (justified by FNN-based logic). In particular, no theoretical analysis was performed for any of the considered dynamical processes (purely deterministic or stochastic).

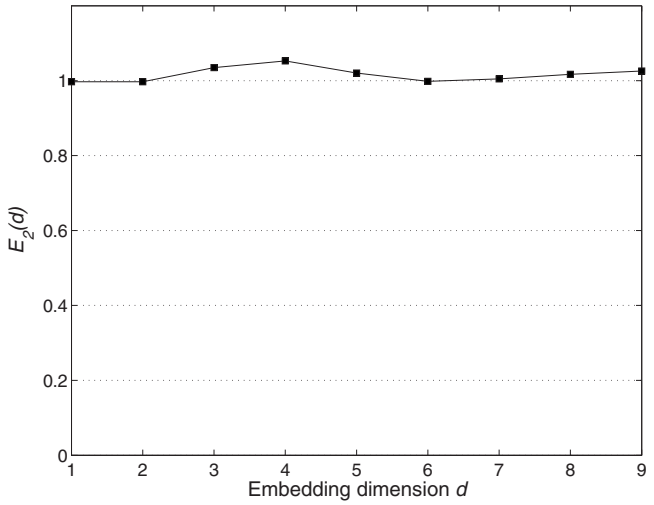

FIG. 4. AFN parameter E_2 as a function of the embedding dimension obtained with a 1000-point simulated colored noise time series generated by an autoregressive AR(1) process (defined by $x_n = 0.95 x_{n-1} + \eta_n$, where η_n are samples of a centered WGN with unit standard deviation). The lag time is $\tau=1$.

In [40], we investigated the statistical properties of the parameter E_2 for a purely random process, namely, a white Gaussian noise (WGN) process. In this case, we have shown that, under some reasonable statistical assumptions, it is possible to derive the two first-order moments of the $E^*(d)$ quantity considered as a random variable which depends on the embedding dimension d. This theoretical result was confirmed by Monte Carlo numerical experiments with 1000 simulated WGN time series. Using some approximations, an estimation of the expected value and standard deviation of the parameter $E_2(d)$ was then performed. These two statistical parameters were respectively shown to be asymptotically equal to 1 and 0.

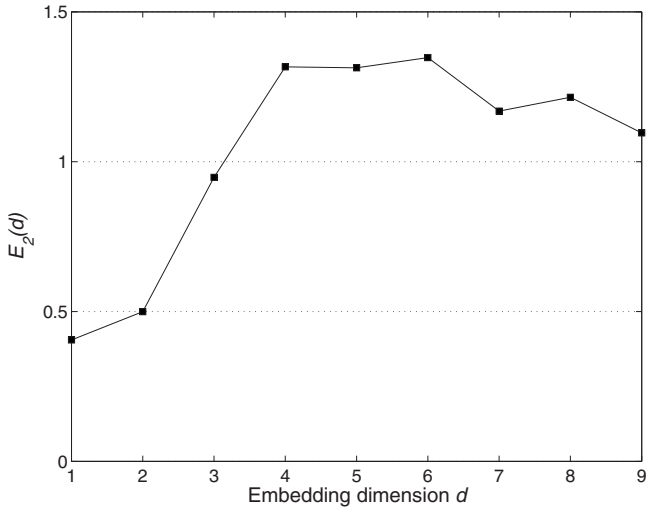

FIG. 5. AFN parameter E_2 as a function of the embedding dimension obtained with a 1000-point x-component Ikeda time series (with lag time $\tau=1$).

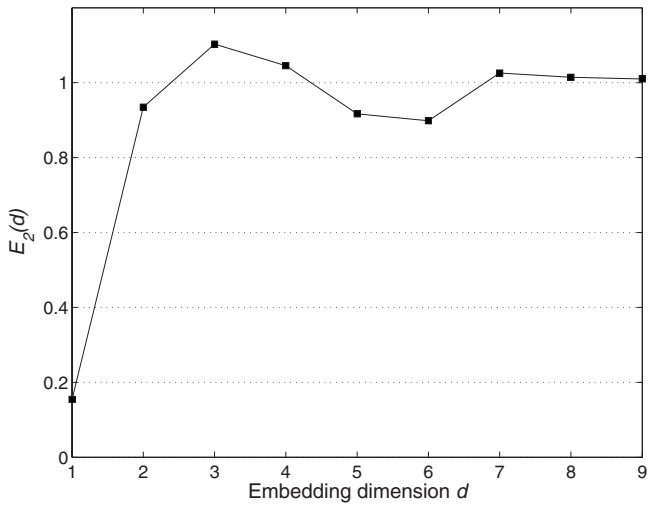

FIG. 6. AFN parameter E_2 as a function of the embedding dimension obtained with a 1000-point x-component Lorenz time series (with lag time $\tau=8$).

This result and the observation of the behavior of E_2 as a function of d naturally led us to propose the estimation of the relative standard error (the normalized standard deviation or variation coefficient) of $E_2(d)$ over a few values of the embedding parameter as a statistic for detecting determinism in short time series. Hence, the criterion is simply defined by the ratio of the standard deviation of $E_2(d)$ to its mean over a fixed d_{max} values of d. We denote it by V_{E_2}.

IV. NUMERICAL EXPERIMENTS

A. General procedure

To assess the efficiency of the criterion, we apply the method to different simulated time series. In the case of deterministic systems (both discrete and continuous), we generate 10 000-sample time series. For the stochastic processes, we simulate 1500-point sequences. In both cases, the time series are then cut into shorter ones of lengths 1000, 500, and 250 points. These shorter sequences are not randomly selected but chosen in order to optimize a certain quantity related to the surrogate data-testing technique (which is detailed in the next section).

In the case of random time series, Monte Carlo tests are performed to quantify the robustness of the V_{E_2} criterion. One hundred realizations of each initial sequence are generated to estimate the efficiency level of the method.

When not specified, the estimation of V_{E_2} is achieved with a d_{max} value of 9, which is a reasonable choice to detect possible low-dimensional deterministic behavior. The only additional parameter needed to perform the test is the time delay τ used for the PSR procedure. For the deterministic time series, we use the first minimum of the AMI function [41]. For the discrete deterministic and stochastic systems, we set τ to 1.

B. Surrogate statistical tests

In order to assess the V_{E_2} statistic, we adopt the surrogate data-testing approach introduced by Theiler *et al.* [20]. In this approach (the AAFT-surrogate-based one), the null hypothesis tested is that the underlying temporal dynamics of the data results from a Gaussian linear stochastic process (which can be modeled by autoregressive moving average processes; see [13] for a detailed discussion).

To achieve this, the criterion is estimated for a fixed number of random time series created from the original data by introducing a subtle stochastic component. Basically, the fast Fourier transform (FFT) of the original time series is computed and then a uniformly distributed random number chosen between 0 and 2π is added to the phase of each of the FFT components to generate a surrogate in the frequency domain. An inverse FFT is then applied to obtain the surrogate time series. The resulting time series have the same statistical parameters and the same Fourier power spectrum (and hence the same autocorrelation function according to the Wiener-Khinchin theorem) as the original data.

More precisely, in the present work, we use improved surrogates: the so-called iteratively refined surrogates proposed by Schreiber and Schmitz [28,29]. Their method corrects deviations in the spectrum and distribution from the goal set by the original data. In other words, the surrogate is filtered toward the correct Fourier amplitudes and rank ordered to the correct distribution. Figures 7–9 show three examples of the simulated time series and their iteratively refined surrogates.

The last step in such a surrogate data testing is to design a statistical test (see [13] for more details). For our criterion, the null hypothesis is associated with the case where the statistic V_{E_2} is likely to be drawn from the distribution defined by the parameters V_{E_2} of the surrogates. A natural approach would be to compute the mean $(m_{V_{E_2}})$ of the V_{E_2} parameter for all the surrogates and its standard deviation $(\sigma_{V_{E_2}})$, and then to verify whether the V_{E_2} parameter of the original time series lies in the interval defined by $[m_{V_{E_2}}-2.58\sigma_{V_{E_2}}, m_{V_{E_2}}+2.58\sigma_{V_{E_2}}]$ (if the test is a two-sided one and for a level of significance $\alpha=0.01$). However, to perform such a test the assumption of a Gaussian distribution of the parameters of the surrogates must be satisfied. For our statistic and at least for the tested time series, it is almost never the case (the Kolmogorov-Smirnov test failed). Hence, we follow Theiler *et al.* [20] and Schreiber and Schmitz [29] and use a simple rank-order test based on the computation of the 100 percentiles of the distribution of the parameters $V_{E_2}$of the surrogates. In order to reach a level of significance $\alpha=0.01$, we generate $2/\alpha-1=199$ surrogates to perform two-sided tests on our simulated time series. The "surrogates" routine of the TISEAN software package [29,42] was used.

An important point that has to be taken into account when generating Fourier-based surrogates is the periodicity artifacts issue. It has been shown [29,43] that a mismatch between the beginning and the end of the time series can lead to important artifacts in the surrogate which can produce spurious rejections of the null hypothesis. To solve this so-called end-to-end mismatch problem, Ehlers *et al.* [44] proposed to extract from the data a subinterval such that the end points match as closely as possible. In the present work, we use a systematic approach proposed by Schreiber and

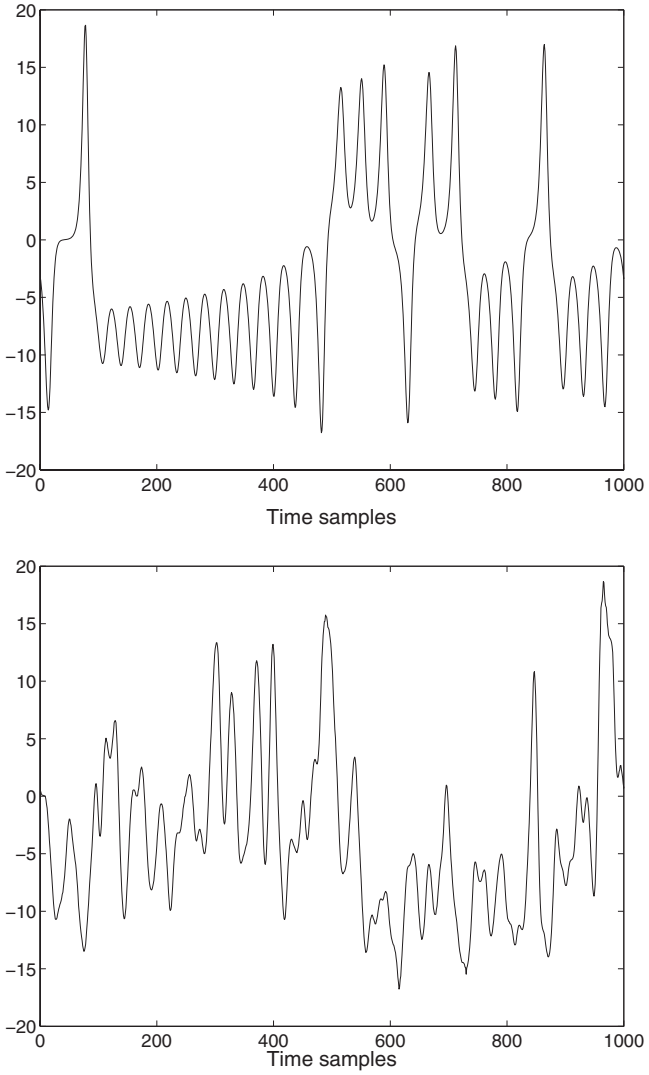

FIG. 7. A 1000-point length simulated Lorenz time series (upper frame) and one of its iteratively refined surrogates (lower frame) obtained by the IAAFT surrogate method.

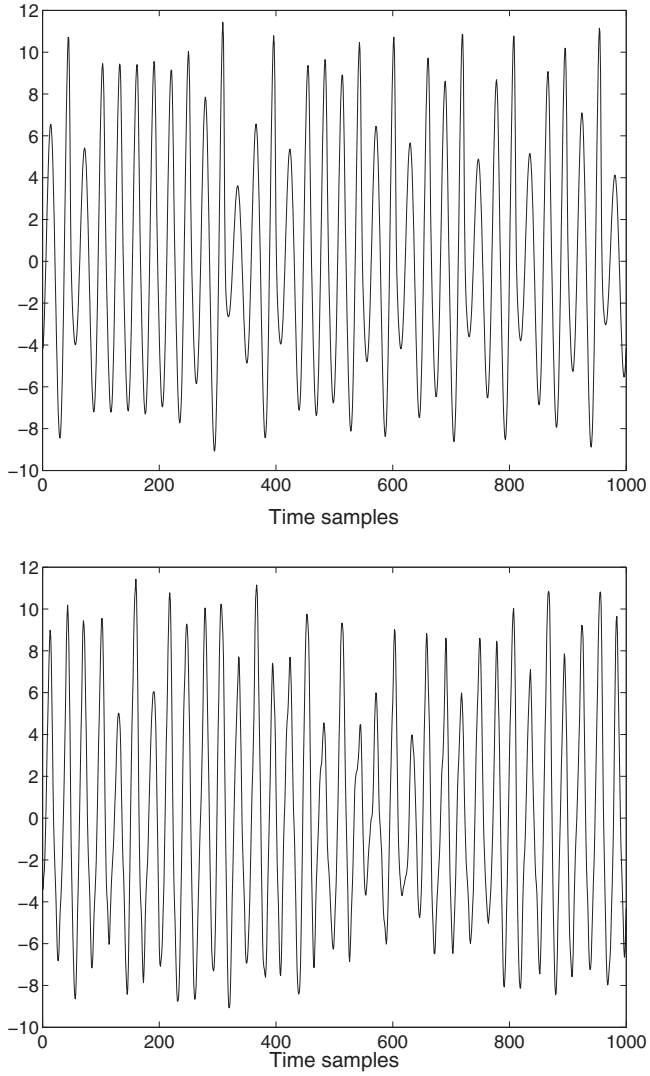

FIG. 8. A 1000-point length simulated Rössler time series (upper frame) and one of its iteratively refined surrogates (lower frame) obtained by the IAAFT surrogate method.

Schmitz [29]. It is based on the minimization of the average of two parameters γ_{jump} and γ_{slip} which quantify, respectively, the end-point mismatch and the first-derivative mismatch. For our numerical experiments and to construct the subsequences described in Sec. IV A, we developed a simple routine (similar to the TISEAN "end to end" routine [42]) which extracts from each initial simulated dataset a time series with a specified length (1000, 500, and 250 samples) which satisfies the minimization of the quantity $(1/2)(\gamma_{jump}+\gamma_{slip})$.

C. The tested models

In this section, we briefly describe the different simulated time series used to assess the efficiency of the criterion. The deterministic data are generated by well known discrete and continuous chaotic systems. A chaotic laser experimental time series is also included in the numerical experiments. Then, some random time series are tested in order to verify that the chosen V_{E_2} statistic is not statistically different from the 199 V_{E_2}'s of the surrogates in this case.

1. Deterministic time series

(a) The Hénon time series. The first deterministic time series presented for these simulations is taken from the Hénon chaotic map [45] defined by

$$x_{n+1} = 1 - ax_n^2 + y_n,$$

$$y_{n+1} = bx_n, \tag{7}$$

with $a=1.4$ and $b=0.3$.

(b) The Ikeda time series. The second chaotic time series presented for these simulations is the x component of the discrete Ikeda attractor [46] defined by

$$x_{n+1} = a + R[x_n \cos(t) - y_n \sin(t)],$$

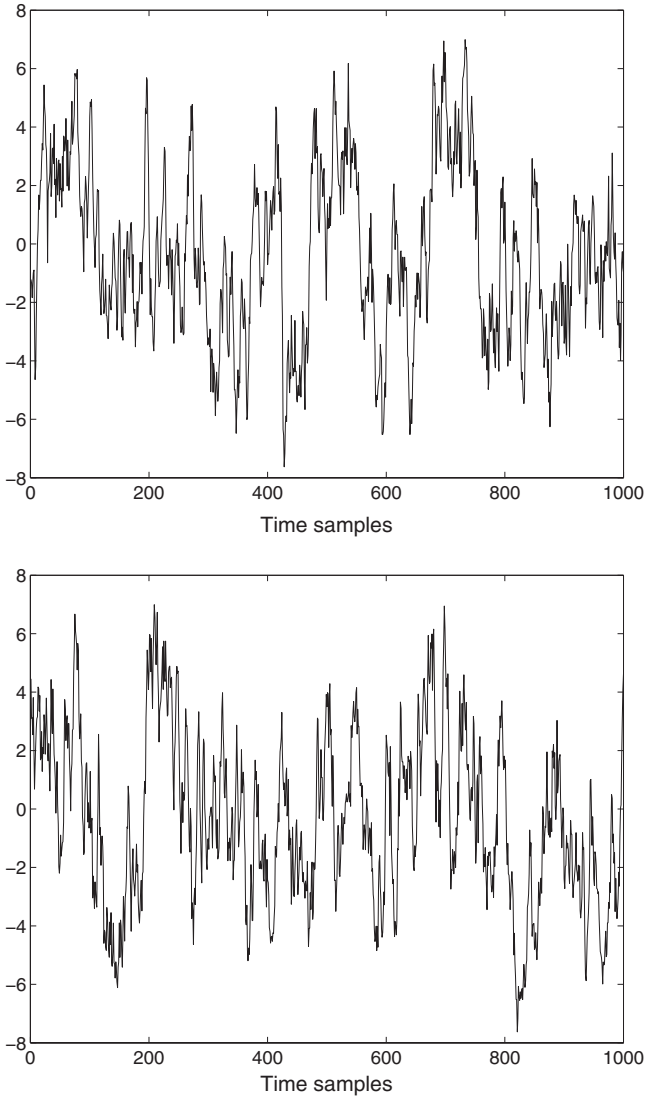

FIG. 9. A 1000-point length simulated colored noise time series generated by an autoregressive AR(1) process (defined by $x_n = 0.95x_{n-1} + \eta_n$, where η_n are samples of a centered WGN series with unit standard deviation, in the upper frame) and one of its iteratively refined surrogates (lower frame) obtained by the IAAFT surrogate method.

$$y_{n+1} = R[x_n \sin(t) + y_n \cos(t)], \tag{8}$$

with $t = \phi - p/(1+x_n^2+y_n^2)$, and the parameters $a=1$, $R=0.9$, $\phi=0.4$, and $p=6$.

(c) The Lorenz time series. For the third numerical experiment, we use the x component of the Lorenz attractor [47] defined by

$$\dot{x} = \sigma(y - x),$$

$$\dot{y} = -xz + \rho x - y,$$

$$\dot{z} = xy - \beta z, \tag{9}$$

with the parameters $\sigma=10$, $\rho=28$, and $\beta=8/3$.

The system is integrated using a fourth-order Runge-Kutta algorithm with integration step 0.02 and unit sampling rate. To get a 10 000-point length dataset, we generate a 15 000-point time series and discard the 5000 first points (to ensure the vanishing of all transients). The lag time τ used to compute the statistic V_{E_2} is estimated via the mutual information method [41]. We obtain $\tau=8$.

(d) The Rössler time series. In this experiment, we use the x component of the Rössler attractor [48] defined by

$$\dot{x} = -(y + z),$$

$$\dot{y} = x + ay,$$

$$\dot{z} = b + (x - c)z, \tag{10}$$

with $a=0.2$, $b=0.2$, and $c=5.7$.

In this case, the system is also integrated using a fourth-order Runge-Kutta algorithm with integration step 0.01 and sampling rate 20. To ensure the vanishing of all transients, we also discard the 5000 first points. Using the AMI function technique, we obtain $\tau=7$.

(e) Laser experimental time series. We use a 10 000-point length experimental dataset from Santa Fe Institute competition NH_3 laser signal. We have chosen this experimental time series because of its known complex dynamical behavior. The laser time series has a Lorenz-like chaotic dynamics [49]. Details of the recording procedure can be found in [65] and also in [13]. The AMI method indicated an optimal lag time $\tau=2$ for the PSR.

2. Stochastic time series

(a) WGN time series. We use data generated by a totally uncorrelated stochastic process having a centered and normalized Gaussian distribution.

(b) Correlated noise time series. We use data generated by a simple AR(1) process defined by

$$x_n = 0.95x_{n-1} + \eta_n, \tag{11}$$

where η_n are samples of a centered WGN series with unit standard deviation.

(c) Random time series with a static nonlinearity. We use again an AR(1) process but we apply a simple nonlinear measurement function as suggested in [13]:

$$s_n = x_n^3,$$

$$x_n = 0.99x_{n-1} + \eta_n, \tag{12}$$

where η_n are also samples of a centered WGN series with unit standard deviation. The aim is to test the criterion on a stochastic time series with a nonlinearity that is not dynamical.

(d) $1/f^{\alpha}$ noise time series. We also include numerical experiments performed on these particular stochastic processes characterized by a power-law-decaying power spectrum.

Among such processes that can be numerically simulated, we have selected examples of fractional Brownian motion (FBM) and fractional Gaussian noise (FGN). The FBM's are

nonstationary fractal processes [50] and their increments are called FGN's. They are characterized by the Hurst exponent H $(0<H<1)$ which specifies the autocorrelation of the processes. The H exponent is theoretically related to the parameter α of the $1/f^{\alpha}$ power spectrum law: $\alpha=2H+1$ in the case of FBM's (in this case we have $1<\alpha<3$) and $\alpha=2H-1$ in the case of FGN's (which correspond to $-1<\alpha<1$). For FBM's, increasing the parameter α smooths the associated time series.

To generate time series of such processes, we use the Cholesky decomposition method (see [51] for instance). This approach is based on the Cholesky decomposition of the covariance matrix of the increments of the FBM process (namely, the associated FGN). Theoretically, it is able to produce exact discrete realizations of a finite-size FGN. The FBM time series (having the same H exponent) is then simply obtained by cumulatively summing the FGN samples.

For our simulations, we select the following cases.

FGN with $H=0.75$ $(\alpha=0.5)$, which corresponds to a long-memory process with a high-frequency global spectral behavior.

FGN with $H=1$ $(\alpha=1)$, which corresponds to the famous $1/f$ or pink noise. This particular stochastic process was used to model physical phenomena [52]. Its statistical properties were also observed in physiology (see [53] for instance, and the references therein).

FBM with $H=0.25$ $(\alpha=1.5)$, which corresponds to a nonstationary process with negatively correlated increments. Such processes are also called antipersistent FBM's.

FBM with $H=0.5$ $(\alpha=2)$, which corresponds to the standard Brownian motion, a nonstationary stochastic Wiener process first described by Brown [54] and then analyzed by Einstein [55].

D. Effect of noise

For the deterministic time series, we also investigate the effect of additive WGN on the results of the method. We add an increasing amount of noise to a 1000-sample subsequence obtained by cutting the 10 000-point initial time series generated by each model [to satisfy the minimization of the quantity $(1/2)(\gamma_{jump}+\gamma_{slip})$]. Technically, the subsequence is first centered and normalized by its standard deviation and then three levels of noise are added. These noises have, respectively, 0.10, 0.30, and 0.50 standard deviations (which correspond to percentages of the standard deviation of the original noise-free subsequence). We also performed Monte Carlo tests using 100 realizations of the added noise time series for each level.

E. Application to a high-dimensional chaotic system

To investigate the results of the chosen criterion on a high-dimensional system, we use a time series generated by the famous Mackey-Glass attractor [56]

$$\dot{x}(t)=\frac{ax(t-\Delta)}{1+x(t-\Delta)^{c}}-bx(t) \tag{13}$$

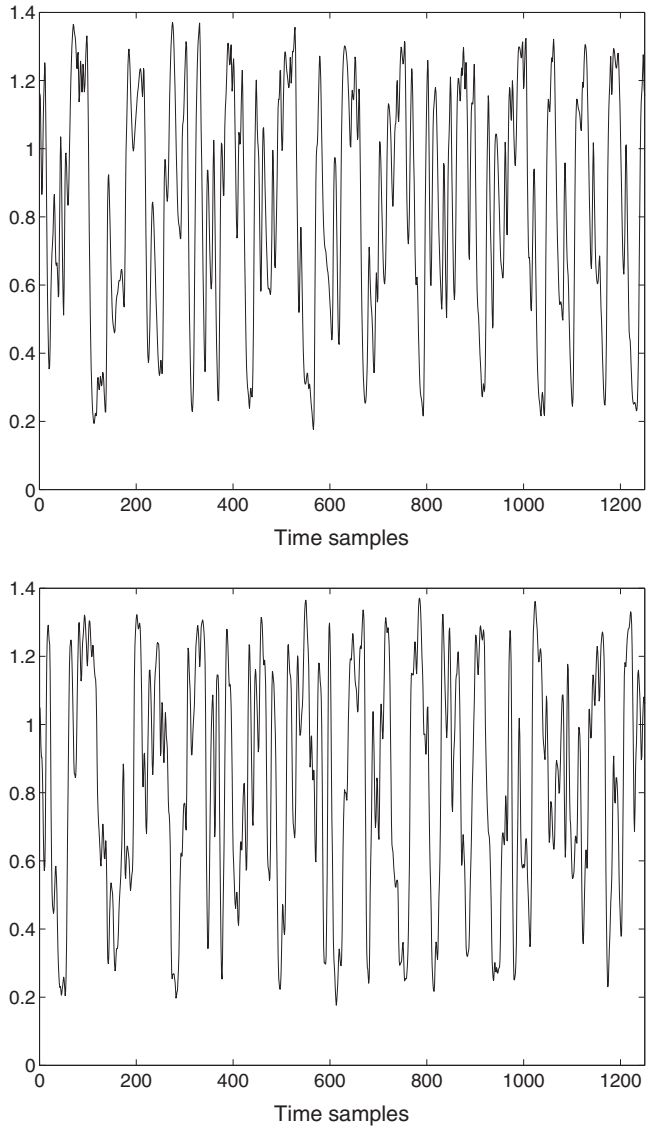

FIG. 10. 1250-point length simulated Mackey-Glass time series (in the upper frame) and one of its iteratively refined surrogates (lower frame).

with $a=0.2$, $b=0.1$, $c=10.0$, and $\Delta=100$. This equation produces a high-dimensional chaotic behavior. The information dimension of the associated attractor can be estimated using the Kaplan-Yorke formula (see [11] and [57]). It is about 10.

Equation (13) is integrated using a fourth-order Runge-Kutta algorithm with integration step 0.01. The sequence obtained is down-sampled and cut to discard the transients, leading to a 2500-point time series. Four subsequences satisfying the end-to-end surrogate mismatch minimization are then extracted. These subsequences have lengths 750, 1000, 1250, and 1500 samples. The 1250-sample one is shown in Fig. 10 with one of its surrogates. We compute the V_{E_2} statistic for the four time series and compare each of them to its 199 surrogate counterparts. The lag time used is $\tau=1$. The d_{max} value is set to 12.

We also investigate the sensitivity to noise of the V_{E_2} statistic for this high-dimensional system. We use the 1250-

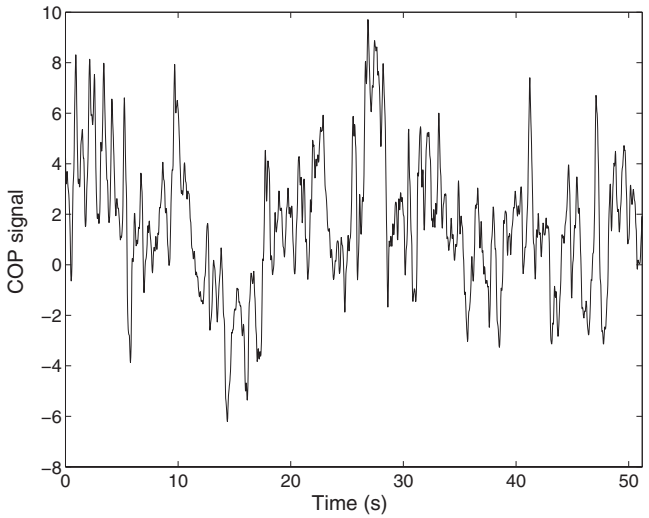

FIG. 11. Human postural sway time series recorded during quiet standing on a force platform. The COP trajectory along the anteroposterior direction is plotted against time.

and 1500-sample subsequences. The procedure is similar to the one used in the previous subsection. The levels of noise are lower: 1% and 10% amounts of WGN are used.

F. Application to postural sway data

Here, we test the criterion on a particular human movement signal, namely, the fluctuations of the center of pressure (COP) measured with a force platform. Such experimental data are often analyzed using different nonlinear or fractal analyses [58–62] or methods from mechanical statistics such as stabilogram diffusion plots [63,64]. The time series used was obtained from the anteroposterior component of the COP during the quiet standing of a healthy elderly human subject. The data were recorded at a sampling rate of 40 Hz and filtered using a lowpass Butterworth filter (fourth order with cutoff frequency 10 Hz). The recording lasted for 51.2 s so the time series is constituted of 2048 samples. It is shown in Fig. 11.

We estimate the V_{E_2} statistic with a lag time $\tau=12$ (provided by the AMI method) and a maximum embedding dimension $d_{max}=12$. We use different subsequences which minimize the effect of the end-to-end mismatch artifact related to the surrogate data-testing procedure. Three different lengths are tested in order to investigate the behavior of the method for such irregular biological time series.

G. Results

The first results of the method are presented in Tables I and II. In these tables, the value of the statistic V_{E_2} is given for each model and time series length. The interval defined by the minimal and maximal V_{E_2} values obtained with the 199 surrogate time series is also given. When the original value is lying inside this interval, the two indices of the percentiles localizing it in the distribution of the surrogate V_{E_2} statistics are given. In Table II, for the random time series, we present the results of one single realization of each process in order to show the global behavior of the algorithm.

In Table III, we show the results of the Monte Carlo simulations obtained with 100 realizations of the stochastic processes. For each of the tested models and times series lengths, we give the rate of successful applications of the surrogate data tests (those for which we cannot reject the null hypothesis). The V_{E_2} parameters means and standard deviations over the 100 realizations are given.

In Table IV, we present the noise effect results obtained for the five deterministic models. The rate of successful surrogate tests is given for each 1000-point time series and for three levels of noise (10%, 30%, and 50% of the standard deviation of the clean sequence).

Tables V and VI show, respectively, the results of the method for the Mackey-Glass system and the rates of suc-

TABLE I. V_{E_2} statistics for the different deterministic series and their surrogate counterparts. The statistic is computed for three different data lengths. The minimal and maximal surrogate values of V_{E_2} are given for each case. When necessary, the indices of the percentiles surrounding the V_{E_2} statistic of the original time series are reported.

	Data length		
Model	1000	500	250
Hénon map	0.3597	0.3562	0.3243
Surrogate statistics [Min, Max]	[0.0159,0.0589]	[0.0156,0.0997]	[0.0246,0.1044]
Ikeda map	0.3417	0.2887	0.1933
Surrogate statistics [Min, Max]	[0.0151,0.0779]	[0.0148,0.0773]	[0.0205,0.1102]
Rössler attractor	0.3722	0.3696	0.3030
Surrogate statistics [Min, Max]	[0.2134,0.2538]	[0.1742,0.2574]	[0.1891,0.2790]
Laser data	0.3381	0.3155	0.3391
Surrogate statistics [Min, Max]	[0.1375,0.2210]	[0.1271,0.2078]	[0.1918,0.2739]
Lorenz attractor	0.3192	0.3250	0.2928
Surrogate statistics [Min, Max]	[0.2253,0.3002]	[0.2363,0.3164]	[0.2572,0.3560]
Percentile indices			20–21

TABLE II. V_{E_2} statistics for the different random time series and their surrogate counterparts. The statistic is computed for three different data lengths. The minimal and maximal surrogate values of V_{E_2} are given for each case. The indices of the percentiles surrounding the V_{E_2} statistic of the original time series are reported.

	Data length		
Model	1000	500	250
WGN	0.0216	0.0338	0.0499
Surrogates statistics [Min, Max]	[0.0107,0.0523]	[0.0180,0.0696]	[0.0215,0.1009]
Percentile indices	21–22	34–35	56–57
Correlated noise AR(1)	0.0250	0.0464	0.0599
Surrogates statistics [Min, Max]	[0.0116,0.0520]	[0.0073,0.0685]	[0.0211,0.1150]
Percentile indices	40–41	76–77	62–63
Correlated noise AR(1) (nonlinear)	0.0354	0.0481	0.0681
Surrogates statistics [Min, Max]	[0.0139,0.0624]	[0.0183,0.0910]	[0.0209,0.1450]
Percentile indices	60–61	68–69	32–33
$1/f^{0.5}$ (FGN with $H=0.75$)	0.0331	0.0363	0.0409
Surrogates statistics [Min, Max]	[0.0119,0.0467]	[0.0169,0.0708]	[0.0163,0.0973]
Percentile indices	75–76	54–55	18–19
$1/f$ (FGN with $H=1$)	0.0251	0.0341	0.0736
Surrogate statistics [Min, Max]	[0.0132,0.0589]	[0.0149,0.0680]	[0.0218,0.1059]
Percentile indices	34–35	40–41	89–90
$1/f^{1.5}$ (FBM with $H=0.25$)	0.0282	0.0421	0.0458
Surrogates statistics [Min, Max]	[0.0078,0.0645]	[0.0162,0.0846]	[0.0249,0.1026]
Percentile indices	49–50	55–56	28–29
$1/f^2$ (FBM with $H=0.5$)	0.0380	0.0503	0.0575
Surrogates statistics [Min, Max]	[0.0126,0.0544]	[0.0171,0.0746]	[0.0258,0.1041]
Percentile indices	86–87	80–81	40–41

TABLE III. The rates of success of the Monte Carlo tests performed on the different stochastic time series. Three different lengths are included and 100 realizations are used for each length and each model. The means and standard deviations of the V_{E_2} statistic over these realizations are also given. Std. dev. indicates standard deviation.

	Data length		
Model	1000	500	250
WGN	100%	99%	97%
V_{E_2} (mean±std. dev.)	0.0274±0.0072	0.0378±0.0090	0.0520±0.0128
Correlated noise AR(1)	97%	99%	100%
V_{E_2} (mean±std. dev.)	0.0271±0.0075	0.0382±0.0088	0.0541±0.0136
Correlated noise AR(1) (nonlinear)	97%	97%	100%
V_{E_2} (mean±std. dev.)	0.0393±0.0110	0.0540±0.0168	0.0684±0.0178
$1/f^{0.5}$ (FGN with $H=0.75$)	97%	98%	97%
V_{E_2} (mean±std. dev.)	0.0269±0.0075	0.0386±0.0100	0.0524±0.0158
$1/f$ (FGN with $H=1$)	100%	98%	97%
V_{E_2} (mean±std. dev.)	0.0270±0.0077	0.0372±0.0108	0.0512±0.0128
$1/f^{1.5}$ (FBM with $H=0.25$)	100%	100%	100%
V_{E_2}(mean±std. dev.)	0.0298±0.0066	0.0381±0.0118	0.0532±0.0142
$1/f^2$ (FBM with $H=0.5$)	97%	97%	97%
V_{E_2} (mean±std. dev.)	0.0287±0.0073	0.0380±0.0099	0.0514±0.0139

TABLE IV. The rates of successful tests in detecting the deterministic nature of the underlying dynamical process of simulated chaotic data corrupted by additive WGN. The Monte Carlo tests were performed on each deterministic time series using 100 realizations of noise. The original sequences are 1000 points and three levels of noise are considered.

	Noise level		
Model	10%	30%	50%
Hénon map	100%	92%	25%
Ikeda map	100%	98%	11%
Rössler attractor	100%	44%	9%
Laser data	100%	59%	2%
Lorenz attractor	90%	85%	11%

cessful tests for detecting its deterministic structure when corrupted by additive noise. Table V includes four different lengths of the time series and Table VI presents the results for two levels of noise added to 1250- and 1500-point Mackey-Glass sequences.

The results of the V_{E_2} statistic for the COP time series are given in Table VII. We present parameters that are similar to those of Table II for three different lengths of the analyzed time series.

V. DISCUSSION AND CONCLUSION

From Tables I and II, we can first observe that the V_{E_2} statistics of the deterministic time series are always higher (about ten times) than the values obtained with the stochastic time series. This is consistent with the AFN algorithm behavior [1,40]. For all the models and all lengths, the surrogate data testing demonstrates the efficiency of the proposed statistic except in one case (the 250-point Lorenz dataset).

From Table I, we also observe that the statistical values of the original simulated deterministic time series decrease globally as we lower the number of available samples. Conversely, the maximal surrogate statistics are increased and get closer to the original V_{E_2} statistics. In this case, and as is naturally expected, the ability of the criterion to discriminate the chaotic behavior is weakened by shortening the data length. Note that this remark does not hold for the laser experimental time series. In this case, the V_{E_2} values are more stable but the deterministic nature of the underlying dynamical process is still revealed even for the 250-point length data.

TABLE VI. The rates of successful tests in detecting the deterministic nature of the underlying dynamical process of the Mackey-Glass data corrupted by additive WGN. The Monte Carlo tests were performed on each deterministic time series using 100 realizations of noise. The original sequences are 1250 and 1500 points in length and two levels of noise are considered.

	Noise level	
Model	1%	10%
Mackey-Glass attractor (1250 points)	86%	13%
Mackey-Glass attractor (1500 points)	93%	12%

For the stochastic time series (see Tables II and III), the original statistics globally decrease when the data length increases. This is consistent with the theoretical result obtained for a WGN in [40] as the asymptotic standard deviation for the parameter $E_2(d)$ is zero for all embedding dimensions. Moreover, we also observe in Table II that both surrogate values defining the [Min, Max] interval are also increased. From Table III, the results show important rates of successful surrogate data tests ranging from 97% to 100%. In all these cases of the Monte Carlo tests, we cannot reject the null hypothesis that the underlying process is a purely stochastic one with a level of significance $\alpha=0.01$. The results also indicate that shortening the time series up to 250 samples has no effect on the efficiency of the method. However, note that, as expected, the variability of the V_{E_2} statistics over the 100 realizations is systematically increased when the number of available samples is decreased.

The results presented in Table IV globally indicate that the V_{E_2} statistic is sensitive to additive noise of 30% intensity or higher. The method performs very well with 10% amount of added noise but failed frequently in some cases (mainly for the Rössler and Laser time series) with 30% level of noise. This sensitivity to noise is not easily detected in the global behavior of the parameter $E_2(d)$ as a function of the embedding dimension d [40]. As argued in Sec. I, the definition of a quantified criterion for the AFN method is necessary and the surrogate data tests allow us to perform a robust test for the noise influence issue. The results of Table IV show also that the V_{E_2} statistic is less sensitive to added noise in the case of discrete chaotic maps such as the Hénon or Ikeda ones. The algorithm is still efficient for a 30% level of

TABLE V. The V_{E_2} statistics obtained for the Mackey-Glass simulated dataset and their 199 surrogate counterparts. The statistic is computed for four different data lengths. The minimal and maximal surrogates values of V_{E_2} are also given. When necessary, the indices of the percentiles surrounding the V_{E_2} statistic of the original time series are reported.

	Data length			
Model	1500	1250	1000	750
Mackey-Glass attractor	0.1980	0.1988	0.1805	0.1793
Surrogate statistics [Min, Max]	[0.1669,0.1883]	[0.1600,0.1893]	[0.1519,0.1877]	[0.1474,0.1824]
Percentile indices			90–91	96–97

TABLE VII. The V_{E_2} statistic for the COP time series and its surrogate counterparts. The statistic is computed for three different data lengths. The minimal and maximal surrogates values of V_{E_2} are given for each length. The indices of the percentiles surrounding the V_{E_2} statistic of the original time series are also reported.

	Data length		
COP data	2000	1000	500
COP data V_{E_2}	0.2112	0.2244	0.2318
Surrogate statistics [Min, Max]	[0.1982,0.2309]	[0.1959,0.2467]	[0.2091,0.2689]
Percentile indices	36–37	53–54	23–24

noise with more than 90% correct detections of the deterministic structure of the time series. For dynamical systems defined by smooth differential equations, the addition of noise creates high-frequency artifacts which lead to spurious rejections of the V_{E_2} statistical tests. This is probably due to the intrinsic geometrical nature of the FNN and AFN algorithms, which are based on the estimation of parameters using the phase-space reconstruction of the possible attractor generating the analyzed data.

The results shown in Table V demonstrate the efficiency of the algorithm for a high-dimensional process. The V_{E_2} statistic is able to distinguish the original time series from its surrogates (with a level of significance of 0.01) with only 1250 available samples (see Fig. 10). We also observe a lower absolute value of the V_{E_2} parameter than those obtained for the lower-dimensional chaotic systems (see Table I). Table VI suggests that the method is more sensitive to noise in this case. With 1% level of added noise, the method is able to detect the deterministic nature of the data but the addition of 10% noise significantly lowers the efficiency of the algorithm. We also observe an increased rate of successful detections (from 86% to 93%) when we extend the number of available samples up to 1500 but only in the case of the 1% level of added noise. Once again, these results bring to light the advantage of the quantified criterion to assess the robustness of this AFN-based approach. The purely graphical original method did not reveal such a sensitivity [40]. This aspect related to the sensitivity to noise for high-dimensional systems surely needs to be investigated in a more detailed manner. The method should be tested for other high-dimensional dynamics time series (possibly by including longer sequences). This point will be studied in further research.

Table VII shows that the analyzed COP experimental time series has a (probably correlated) random structure whatever the length of the tested subsequence. We observe that the V_{E_2} values are much larger than those of the simulated stochastic time series. This suggests that a single computation of the V_{E_2} statistic for the original data (without comparing it to the surrogate ones) cannot be used to obtain reliable information on the nature of the underlying process. Moreover, as for the simulated stochastic time series, the V_{E_2} parameter is increased when we decrease the number of available samples. This result is consistent with the findings of some studies on similar data [60,63,64] as one of the theoretical models proposed for the description of postural sway time series is an antipersistent fractional Brownian motion. Some other authors [58,59,61] proposed a high-dimensional deterministic chaotic or nonlinear structure to describe these fluctuations. Nevertheless, this interpretation of the COP signal nature seems to fail when a proper analysis [62] is applied to long COP time series (12 000 points) by estimating correlation dimensions or largest Lyapunov exponents. However, these long COP sequences were obtained from oversampled raw data that were low-pass-filtered afterward. The time scale issues produced by such a procedure are not easy to solve. Nevertheless, to our knowledge, there is no rigorous scientific evidence of deterministic chaos in experimental COP data. We can conclude that the results of our approach are in agreement with the most common (stochastic) model proposed in the COP dynamics state of the art.

The method proposed in this paper showed interesting results for short time series, including a high-dimensional one. From a purely qualitative point of view, it has some methodological advantages when compared to other approaches described in the Introduction. For instance, many of these algorithms [4,21,23,24,26,27,30–32] require input parameters such as a threshold radius or an accurate minimum embedding dimension to provide good performance. Some others are purely graphical [1,19] and do not propose any quantified output parameter that can be statistically tested. From a more quantitative point of view, we have compared our approach to a smoothness-analysis-based method, namely, the Jeong *et al.* one [26,27]. This method is designed for short time series and is computationally very efficient. The authors have tested their method on 2000-point time series generated by the Van der Pol, Lorenz, and Rössler systems, and also by a high-dimensional system constituted of several coupled well-known nonlinear dynamical systems. They also used a $1/f$ noise data to assess their statistic: the central tendency measure of the cosines of the angles between successive directional vectors in the reconstructed phase space (see Sec. I and Fig. 1). This method (combined with the surrogate data-testing procedure described in Sec. IV B) showed equivalent results to ours for the stochastic time series described in Sec. IV C 2. We used Monte Carlo tests (with 100 realizations of each random simulated dataset) and globally obtained similar rates of successful tests for which the null hypothesis of a stochastic underlying process cannot be rejected. This was done with 250-sample sequences. The only significant difference between the methods was related to the AR(1) process with cubic nonlinearity: the CTM statistic produced a rate of 88% successful tests

whereas the V_{E_2} one gave a rate of 100% (see Table III). The results obtained with the COP time series were consistent with those of the V_{E_2} parameter. For the Lorenz and Rössler time series, the CTM statistic also succeeded in detecting the deterministic dynamics (even with 250-point sequences). In addition, we tested this approach for the Hénon and Ikeda simulated time series. Despite the smoothness of the reconstructed trajectories of these discrete chaotic systems, the proposed CTM statistic (see Fig. 1) failed to discriminate the deterministic structure of the underlying process for some lengths of the considered sequences (250 samples for the Hénon map and all the lengths for the Ikeda one). For the Mackey-Glass data, this method also failed even with a 2000-point time series. The CTM statistics of the original subsequences were never statistically different from their 199 surrogate counterparts. This smoothness-detection-based method seems to produce spurious results for very irregular high-dimensional time series generated by delayed ordinary differential equations such as the Mackey-Glass one. It is also unable to detect determinism in fast bursting dynamics data [27] such as the laser set. However, it shows a good robustness to additive noise in some cases. Indeed, it can be applied successfully [26] with a 100% level of added white noise to a 2000-point time series generated by a continuous system such as the Lorenz one. Finally, we would like to underline the fact that the absolute CTM parameter value is strongly dependent on the choice of the embedding dimension and the lag time used for the PSR.

As a conclusion, we have presented in this paper a criterion for distinguishing purely deterministic time series from random ones (including correlated noise). The proposed statistic is derived from a quantity stated by the AFN method [1], which is a modified version of the FNN approach [4] for detecting determinism. Our approach has two main advantages compared to others: it is quite simple to implement and it is efficient for short datasets such as 250-point length time series. Its sensitivity to noise is acceptable for many applications. This computationally efficient method (associated with the IAAFT surrogate data testing) require only the PSR lag time as an input parameter.

ACKNOWLEDGMENT

The authors would like to thank Dr. Pierrick Bernard for providing the experimental COP data.

[1] L. Cao, Physica D **110**, 43 (1997).
[2] N. H. Packard, J. P. Crutchfield, J. D. Farmer, and R. S. Shaw, Phys. Rev. Lett. **45**, 712 (1980).
[3] F. B. Takens, in *Dynamical Systems and Turbulence*, edited by D. A. Rand and L. -S. Young, Lecture Notes in Mathematics Vol. 898 (Springer, Berlin, 1981), p. 366.
[4] M. B. Kennel, R. Brown, and H. D. I. Abarbanel, Phys. Rev. A **45**, 3403 (1992).
[5] P. Grassberger and I. Proccacia, Physica D **9**, 189 (1983).
[6] M. Sano and Y. Sawada, Phys. Rev. Lett. **55**, 1082 (1985).
[7] A. Wolf, J. Swift, H. Swinney, and J. Vastano, Physica D **16**, 285 (1985).
[8] J.-P. Eckmann, S. O. Kamphorst, D. Ruelle, and S. Ciliberto, Phys. Rev. A **34**, 4971 (1986).
[9] M. Rosenstein, J. Collins, and C. D. Luca, Physica D **65**, 117 (1993).
[10] P. Grassberger and I. Procaccia, Phys. Rev. A **28**, 2591 (1983).
[11] J.-P. Eckman and D. Ruelle, Rev. Mod. Phys. **57**, 617 (1985).
[12] S. Pincus, Proc. Natl. Acad. Sci. U.S.A. **88**, 2291 (1991).
[13] H. Kantz and T. Schreiber, *Nonlinear Time Series Analysis* (Cambridge University Press, Cambridge, 1997).
[14] H. Abarbanel, *Analysis of Observed Chaotic Data* (Springer-Verlag, New York, 1996).
[15] S. Sugihara and R. May, Nature (London) **344**, 734 (1990).
[16] A. Tsonis and J. Elsener, Nature (London) **358**, 217 (1992).
[17] M. B. Kennel and S. Isabelle, Phys. Rev. A **46**, 3111 (1992).
[18] D. T. Kaplan and L. Glass, Phys. Rev. Lett. **68**, 427 (1992).
[19] R. Wayland, D. Bromley, D. Pickett, and A. Passamante, Phys. Rev. Lett. **70**, 580 (1993).
[20] J. Theiler, S. Eubank, A. Longtin, B. Galdikrian, and J. Farmer, Physica D **58**, 77 (1992).
[21] L. W. Salvino and R. Cawley, Phys. Rev. Lett. **73**, 1091 (1994).
[22] J. Jeong, M. S. Kim, and S. Y. Kim, Phys. Rev. E **60**, 831 (1999).
[23] G. J. Ortega and E. Louis, Phys. Rev. Lett. **81**, 4345 (1998).
[24] G. J. Ortega and E. Louis, Phys. Rev. E **62**, 3419 (2000).
[25] G. J. Ortega, C. Degli Esposti Boschi, and E. Louis, Phys. Rev. E **65**, 016208 (2001).
[26] J. Jeong, J. Gore, and B. Peterson, IEEE Trans. Biomed. Eng. **49**, 1374 (2002).
[27] J. Jeong, J. Gore, and B. Peterson, Biol. Cybern. **86**, 335 (2002).
[28] T. Schreiber and A. Schmitz, Phys. Rev. Lett. **77**, 635 (1996).
[29] T. Schreiber and A. Schmitz, Physica D **142**, 346 (2000).
[30] M. Barahona and C. Poon, Nature (London) **381**, 215 (1996).
[31] J. Bhattacharya and P. Kanjilal, Physica D **132**, 300 (1998).
[32] T. Gautama, D. Mandic, and M. V. Hulle, Physica D **190**, 167 (2004).
[33] D. R. Fredkin and J. A. Rice, Phys. Rev. E **51**, 2950 (1995).
[34] C. Rhodes and M. Morari, Phys. Rev. E **55**, 6162 (1997).
[35] T. Aittokallio, M. Gyllenberg, J. Hietarinta, T. Kuusela, and T. Multamaki, Phys. Rev. E **60**, 416 (1999).
[36] C. J. Celluci, A. M. Albano, and P. E. Rapp, Phys. Rev. E **67**, 066210 (2003).
[37] S. P. Garcia and J. S. Almeida, Phys. Rev. E **71**, 037204 (2005).
[38] T. P. Lim and S. Puthusserypady, Phys. Rev. E **72**, 027204 (2005).
[39] R. Hegger and H. Kantz, Phys. Rev. E **60**, 4970 (1999).
[40] S. Ramdani, J.-F. Casties, F. Bouchara, and D. Mottet, Physica D **223**, 229 (2006).
[41] A. M. Fraser and H. L. Swinney, Phys. Rev. A **33**, 1134 (1986).

[42] R. Hegger, H. Kantz, and T. Schreiber, Chaos **9**, 413 (1999).
[43] J. Theiler, P. Linsay, and D. Rubin, in *Time Series Prediction: Forecasting the Future and Understanding the Past*, edited by A. S. Weigend, and N. A. Gershenfeld, Santa Fe Institute Studies in the Science of Complexity, Proceedings Vol. XV (Addison-Wesley, Reading, MA, 1993).
[44] C. Ehlers, J. Havstad, D. Prichard, and J. Theiler, J. Neurosci. **78**, 7474 (1998).
[45] M. Hénon, Commun. Math. Phys. **50**, 69 (1976).
[46] K. Ikeda, Opt. Commun. **30**, 257 (1979).
[47] E. Lorenz, J. Atmos. Sci. **20**, 130 (1963).
[48] O. Rossler, Phys. Lett. **57A**, 397 (1976).
[49] H. Haken, Phys. Lett. **53A**, 77 (1975).
[50] B. Mandelbrot and J. van Ness, SIAM Rev. **10**, 422 (1968).
[51] T. Lundahl, W. Ohley, S. Kay, and R. Siffert, IEEE Trans. Med. Imaging **5**, 152 (1986).
[52] B. Mandelbrot, IEEE Trans. Inf. Theory **13**, 289 (1967).
[53] J. M. Hausdorff and C.-K. Peng, Phys. Rev. E **54**, 2154 (1996).
[54] R. Brown, Philos. Mag. **4**, 161 (1828).
[55] A. Einstein, Ann. Phys. **17**, 549 (1905).
[56] M. Mackey and L. Glass, Science **197**, 287 (1977).
[57] M. Casdagli, Physica D **35**, 335 (1989).
[58] N. Yamada, Hum. Mov. Sci. **14**, 711 (1995).
[59] M. Riley, R. Balasubramaniam, and M. Turvey, Gait and Posture **9**, 65 (1999).
[60] A. Sabatini, Med. Biol. Eng. Comput. **38**, 617 (2000).
[61] P. Pascolo, A. Marini, R. Carniel, and F. Barazza, Chaos, Solitons Fractals **24**, 1343 (2005).
[62] P. Pascolo, F. Barazza, and R. Carniel, Chaos, Solitons Fractals **27**, 1339 (2006).
[63] J. Collins and C. D. Luca, Exp. Brain Res. **95**, 308 (1993).
[64] J. J. Collins and C. J. De Luca, Phys. Rev. Lett. **73**, 764 (1994).
[65] http://www-psych.stanford.edu/~andreas/Time-Series/SantaFe.html